2014 IEEE International Conference on Robotics & Automation (ICRA)
Hong Kong Convention and Exhibition Center
May 31 - June 7, 2014. Hong Kong, China

Robotic Implant to Apply Tissue Traction Forces in the Treatment of Esophageal Atresia

Dana D. Damian, *Member, IEEE*, Slava Arabagi, Assunta Fabozzo, M.D., Peter Ngo, M.D., Russell Jennings, M.D., Michael Manfredi, M.D., and Pierre E. Dupont, *Fellow, IEEE*

***Abstract*— This paper introduces robotic implants as a novel class of medical robots in the context of treating esophageal atresia. The robotic implant is designed to apply traction forces to the two disconnected esophageal segments to induce sufficient growth so that the two ends can be joined together to form a functioning esophagus. In contrast to the current manual method of externally applying traction forces, the implant offers the potential to avoid prolonged patient sedation and to substantially reduce the number of X-rays required. A prototype design is presented along with evaluation experiments that demonstrate its capabilities to apply traction forces to ex vivo esophageal tissues.**

I. INTRODUCTION

Surgical robots have yielded benefits in medicine by augmenting the surgeon's physical capabilities while enabling the integration of multi-modal imaging and sensory data [1]. The greatest potential impact is when the use of robotics in comparison with manual surgery results in both reduced invasiveness together with superior outcomes. Towards reducing invasiveness, medical robots are being designed that move inside the body without reliance on a rigid mechanical connection outside the patient. Examples include tethered mobile robots such as Heartlander that can perform localized sensing, mapping and treatment over the entire surface of the heart [2]. Another class of examples is the tethered intestinal crawlers designed to increase the capabilities of colonoscopy while simultaneously reducing its trauma [3] [4] [5]. In addition, tetherless unactuated smart pills incorporating wireless cameras and other sensors have opened up new directions in medical diagnostics [6] [7] [8] [9] [10].

A completely new category of medical robot that has yet to be explored is that of robotic implants. This field characterizes robots that autonomously regulate biological processes inside the body for long periods of time. The benefits of robotic implants are multiple: they remove the necessity of repetitive surgical interventions, and consequent infection risks and pain, while restoring degraded or missing biological functionalities. While they may move through the body, they may also reside in one location and employ their degrees of freedom to interact with tissue structures. For example, they could perform such tasks as adjusting flow rates through valves and organs or act to change the length or compliance of tissues.

*This work was supported by Swiss National Science Foundation grant PBZHP2_143344.

D.D. Damian, S. Arabagi, A. Fabozzo, P. Ngo, R. Jennings, M. Manfredi and P. Dupont are with Boston Children's Hospital, Harvard Medical School, Boston, U.S.A. dana.damian@childrens.harvard.edu

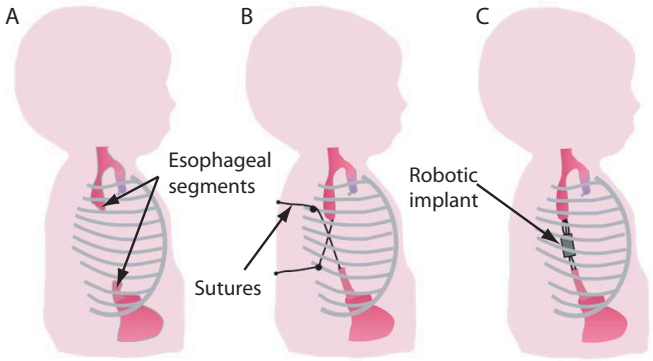

Fig. 1. Inducing tissue growth through traction forces. A. Long-gap esophageal atresia. B. Current treatment uses sutures looped around ribs and tied off outside back. C. Proposed robotic implant.

One example for which a robotic implant would be extremely beneficial is esophageal atresia (EA). This is a congenital defect afflicting about 1000 babies per year in the US, in which the ends (segments) of the esophagus are not connected (see Fig. 1A). Other applications include conditions where lengthening of tubular structures is desired, such as the bowel and the vasculature [11]. If the gap between the two ends is small, they can be surgically connected. When the gap is 3cm or more, however, it is not possible to stretch the tissue sufficiently to create a connection. For these cases, known as long-gap esophageal atresia (LGEA), the best current solution consists of applying traction forces to each end of the esophagus for 14 days in average (Foker's technique) [12] [13]. This causes each end of the esophagus to grow (lengthen) in the direction of the forces. When sufficient lengthening is achieved, the two ends are surgically connected. As shown in Fig. 1B, the traction forces are currently applied using sutures that are looped around the ribs and tied off outside the patient's back. Every day the sutures are manually tightened and X-ray imaging is used about every other day to assess tissue lengthening and to check for potential suture tear out.

While producing superior outcomes to alternative procedures, the child is sedated and kept on a ventilator for the duration of the treatment. Sedation is necessary to avoid motion of the rib cage that occurs during arm movement as it may lead to tearing out the traction sutures. It would be extremely beneficial to these patients if (1) multi-week sedation could be avoided so as to eliminate any effect on long-term neurocognitive development, (2) X-ray imaging

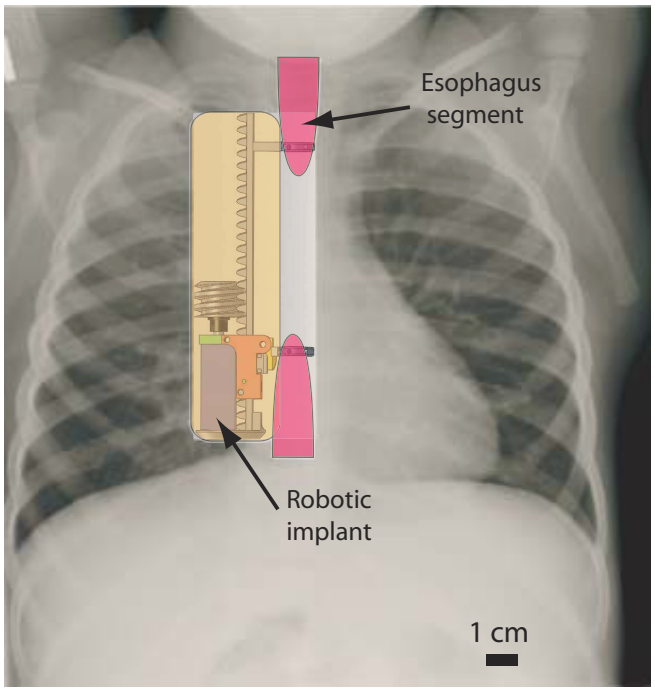

Fig. 2. Positioning of robotic implant within the chest.

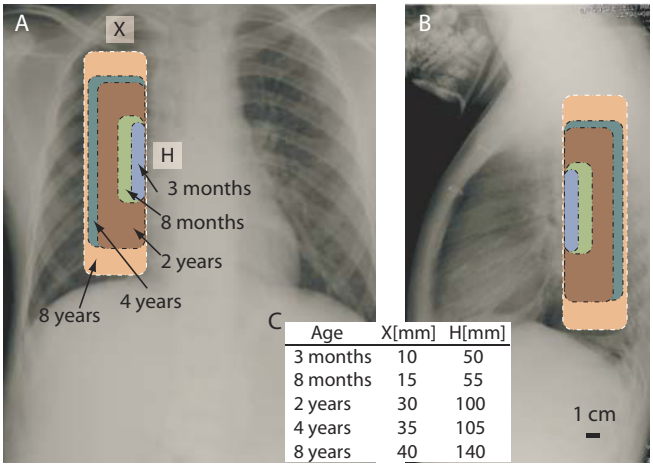

Fig. 3. Available space for robotic implant shown on X-ray image of eight year old patient. A. Front view. B. Lateral view. C. Clinical estimate of volume available based on patient age.

to verify progress could be reduced or eliminated, and (3) the need for re-operation due to suture tear out could be reduced. A robotic implant has the potential to resolve these shortcomings. As depicted in Fig. 1C, such a device could apply tension to both ends of the esophagus simultaneously. Since sutures are no longer tensioned around ribs, the patient could avoid sedation. In addition, tissue lengthening and force could be monitored and controlled using implant sensors reducing the need for X-rays while also enabling more precise control of traction forces.

The contribution of this paper is to propose, fabricate and perform initial testing of a robotic implant for treating LGEA. Section II describes alternate approaches to treating LGEA. Section III presents design requirements and implant design. Calibration and evaluation experiments appear in Section IV and conclusions are given in the final section.

II. Related work

The repair of LGEA is considered one of the most difficult surgical interventions in pediatrics. A number of surgical procedures are being applied in order to restore the structure and functionality of the esophagus [14]. Some LGEA treatments aim to complete the esophagus using a surrogate tissue for the missing segment. Colonic, gastric and jejunal graft interposition are among the most popular [15] [16]. However, there is a general agreement that using the patient's own esophagus should lead to superior results compared to any esophageal replacement [14].

The long gap between the two esophageal segments led to the development of techniques that attempt to stretch the segments and finally connect the two ends (anastomosis). A widely used method of lengthening the esophageal segments is circular myotomy, which proposes the elongation of the highly stretchy submucosal layer of the esophagus in order to bring the segments together [17]. However, because this layer is highly stretched, while the other layers are divided and not included in the anastomosis, the method leads to leaks and other complications at the myotomy sites.

A different LGEA technique uses a multistaged extrathoracic elongation process of the esophagus segments [18] [19] [20]. This method involves making sequential skin incision sites to which the esophagus segment is connected under tension, until its length is sufficient to perform anastomosis.

Lengthening the esophagus axially is an alternate viable approach. This has been attempted using magnetic forces, e.g., electromagnetic bougienage [21], hydraulically controller magnetic forces [22]. Although axial traction is mechanically advantageous in the LGEA, the magnets tend to erode the esophagus internal tissue where they reside, due to increasing attraction magnetic forces, leading to the risk of magnet evasion into the body.

Foker's technique, as described in the previous section, has been used in numerous cases and relies on manual and periodic application of traction forces on sutures loops that are attached to the esophagus segments [12] [13] [23]. Over the course of a couple of weeks, suture tension is adjusted daily to induce lengthening of the esophageal segments through two incision sites on the patient's back. While a successful technique for cases of varying complexity, the approach has several shortcomings as described earlier. These include the need for multi-week sedation, frequent X-rays to assess progress and the potential for the (typically) four pledgeted suture loops to tear out of a segment necessitating re-operation. Furthermore, the elongated tissue has a reduced lumen size (stricture) potentially because of the "necking" that occurs with the current suture attachment method. The robotic implant introduced here is based on Foker's technique and its design is intended to address these shortcomings.

TABLE I
IMPLANT DESIGN REQUIREMENTS

Requirements	Value	Unit
Maximum force	4	N
Maximum gap size	45	mm
Targeted child age	2	years

III. ROBOTIC IMPLANT DESIGN

The concept for the robotic implant is depicted in Fig. 2. In the proposed approach, a motorized implant will apply equal and opposite forces to the two esophageal segments. It will be positioned on the right side of the chest, away from the heart and displace a small portion of the volume normally filled by the right lung. In the anterior-posterior direction, it will be positioned so as to avoid compression of the main stem bronchus. To avoid the need for sedation, the device will not be attached to the ribs, but instead will be "floating" in the chest, supported by the esophageal segments and surrounding tissue.

These clinical considerations regarding implant positioning, as well as the age of the child, are determining factors for the space available for the robotic implant. An estimation of the available space is listed in Fig. 3C. Miniaturization is one of several challenges in prototype design. The approach taken here was to develop a device sized for a two-year-old patient and in future versions reduce its size for younger patients. Furthermore, while it may be possible to create a wireless implant in the future, it is assumed here that a cable will exit the patient's chest to supply power and communication signals.

While the effect of force variation with time on tissue lengthening is not known, the clinical evidence suggests that the current approach of increasing force once a day and then allowing the tissue to relax is effective. By incorporating both force and position sensors in the implant, traction force can be programmed to replicate current clinical practice while also monitoring tissue lengthening. In this manner, X-ray monitoring can be significantly reduced.

Preliminary experiments to measure applied suture forces indicate forces are in the range of 2-4N. For these cases, the sutures were subjected to significant friction because they were pulled out of the body. These traction forces were sufficient to elongate the tissue about 5mm per day [24]. In the technique described in [22], the axial traction force on the esophagus was 0.5N. Regarding the gap between the two esophageal segments, a typical gap size is 45mm, though it can also reach up to 100mm. Based on these considerations, the force production and sensing specifications for the implant were set at 5N while the travel and position sensing distance was set to 45mm. The design specifications are summarized in Table I.

The current method of suture attachment to esophageal segments using pledgeted suture loops is illustrated in Fig. 4A [23]. The proposed alternative method of attachment to the robotic implant appears in Fig. 4B. In the proposed approach, the tissue is sutured to a rigid ring such that the traction force is distributed more uniformly to the tissue and, furthermore, esophagus diameter is maintained with the goal of avoiding the "necking" and stricture inherent in the current approach.

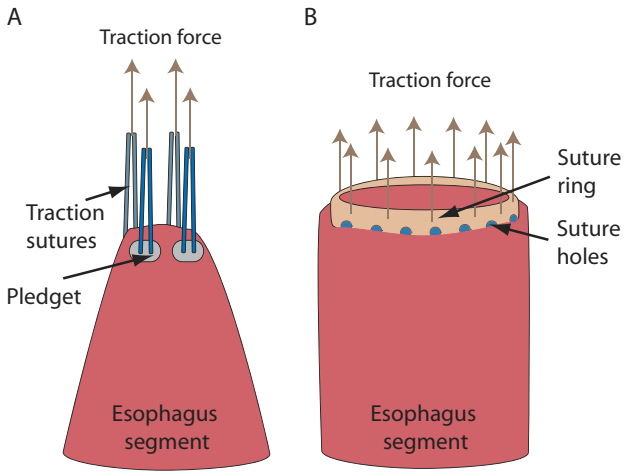

Fig. 4. Suture attachment methods. A. Standard method using four pledgeted suture loops. B. Proposed attachment method using ring to which tissue is sutured.

A. Implant design

To replicate manual force application, the implant should be capable of applying a desired force and then holding the actuator position associated with that force until the next adjustment time. The proposed robotic implant automates the tissue lengthening process.

The non-continuous manual traction operation currently performed on the esophagus requires an automatic mechanism that can hold the position of the esophagus segment for most of the time and actuate in short time bursts. This suggests the use of a nonbackdrivable transmission which was implemented using a rack and worm gear combination as shown in Fig. 5. The worm gear is coupled to a DC motor and mounted on an aluminum car sliding on a polymer rack reinforced with an embedded steel rod. As shown, the length of the rack is 6cm, but this can be adjusted for different LGEA gaps.

The esophageal segments are sutured to the two rings mounted on the rack and sliding car, which are brought together as the worm moves along the rack. Distance between the rings is measured using a linear potentiometer mounted on the rack (Tekscan, Inc.) and ring force is measured using a sensor (Honeywell, Inc) mounted on a freely rotating hinge, as shown in Fig. 5A,B. Because the implant will be loosely sutured to the chest wall to support its weight, the effect of the implant's mass on the force sensor will be minimized.

B. Encapsulation

A compliant waterproof encapsulation was developed to isolate the mechanical and electrical components of the robotic implant from the surrounding tissue. The encapsulation must have sufficient rigidity to exclude surrounding tissue and yet be sufficiently compliant to prevent tissue

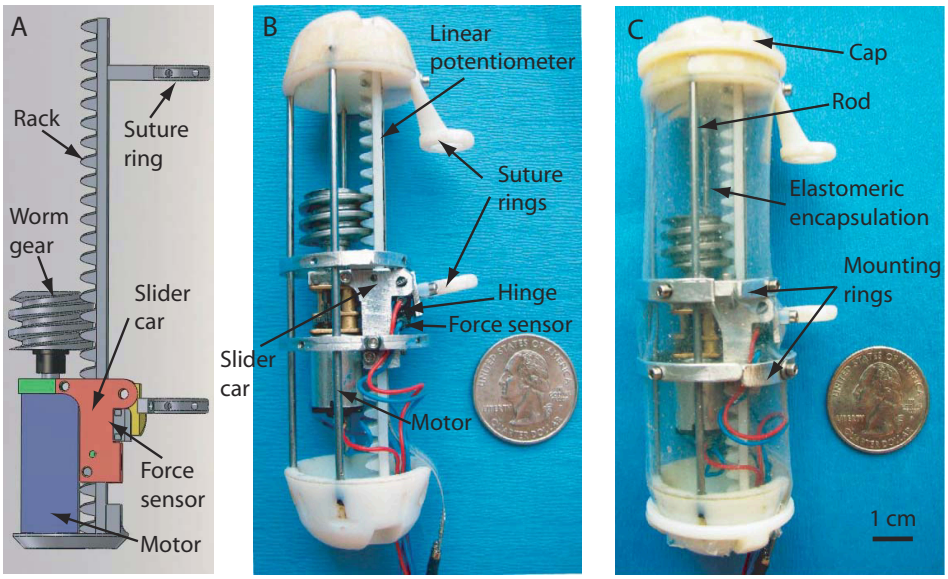

Fig. 5. Robotic implant. A. CAD schematic. B. Implant without elastomeric sleeve. C. Encapsulated implant.

damage. To achieve these aims, the encapsulation structure consists of a stiff internal skeleton and a soft elastomer sleeve as shown in Fig. 5C.

The internal skeleton consists of three longitudinal steel rods, two aluminum rings that act as elastomer membrane fixing anchors, and two polymer end caps to secure the ends of the elastomer membrane. An outer compliant cylindrical sealing sleeve (Ecoflex 00-30, Smooth-On, Inc.) covers the entire robotic implant except for the two suture rings. The sleeve is manufactured by first curing a flat 1.5mm thick sheet on a flat surface, and then wrapping it around a 30mm wide cylinder, while sealing the edges with identical elastomer.

The resulting soft sleeve is fixed to the two end caps of the implant, as well as to the two mounting rings on the slider car by means of a compression clamp, in order to reduce risks of tear outs due to holes created by screws. Furthermore, the two mounting rings serve to eliminate any stresses on the elastomeric sleeve due to slider car motion, in order to prevent any effect on the force sensor measurements. The steel longitudinal rods are lubricated before encapsulation to promote sliding of the sleeve during actuation. The encapsulated implant is 100mm long with a diameter of 30mm and a mass of 55g.

C. Controller design

The control task is to drive suture ring force to a specified set point and then hold the corresponding position while monitoring force and position over time. Thus, the motor is activated only during force set point control and the nonbackdrivability of the rack and gear transmission is used to hold gap distance fixed between actuation cycles. As shown in Fig. 6, the controller was implemented using a Baby Orangutan 328P Board (Pololu Corp.), equipped with an Atmel microcontroller, a motor driver, and serial communication capabilities. The board acquires data from

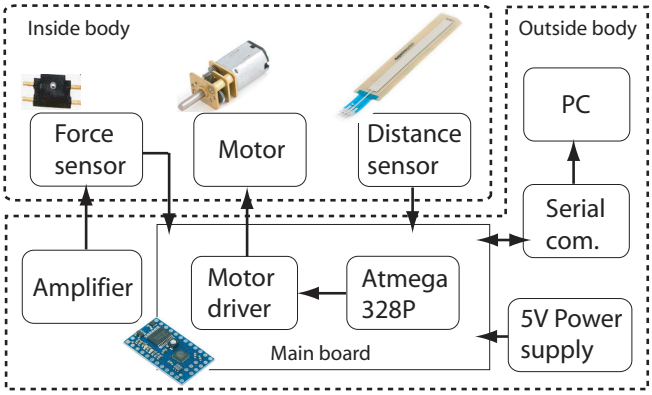

Fig. 6. Controller schematic. The "Inside body" label designates the electronics that are incorporated in the robotic implant, while the "Outside body" label denotes the electronics that would currently reside outside the body of the patient.

the linear potentiometer and force sensor at 200Hz and transmits it to an external PC via USB. The force signal is amplified and filtered using a low pass filter with a cutoff frequency of 22.7Hz. Force control was implemented, in which the force reference control is set from the PC and transmitted to the board through serial communication. An overdamped proportional controller is used to avoid traction force overshoot during set-point adjustment.

IV. Experiments

A sequence of experiments were performed to evaluate the prototype implant. These involved calibrating the position and force sensors as well as demonstrating that the desired maximum traction force could be achieved. In addition, ex vivo experiments were performed with porcine esophageal tissue to evaluate the force controller. To simplify testing, the robotic implant was suspended by its upper suture ring, as shown in Fig. 7, from stiff frame. Loads were applied to

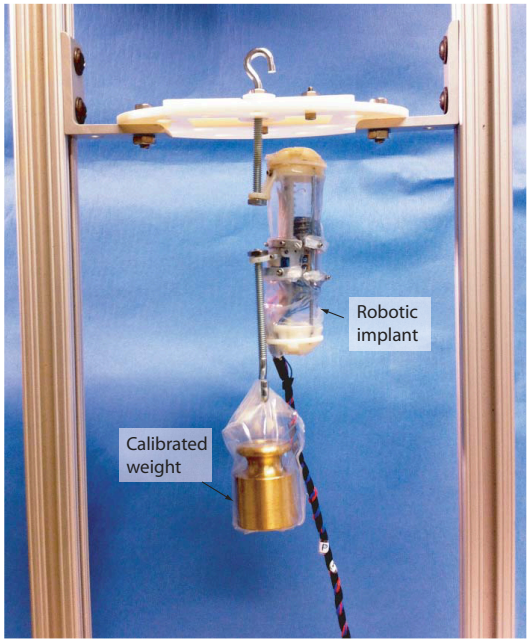

Fig. 7. Experimental setup for sensor calibration.

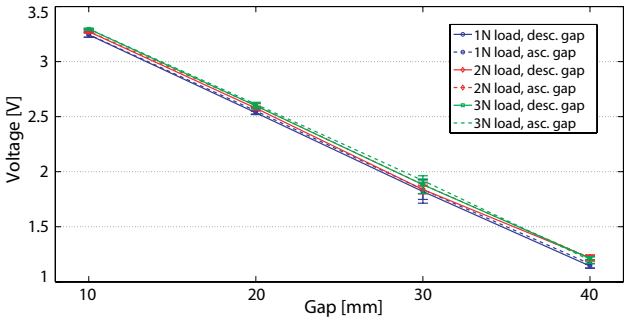

Fig. 8. Distance sensor calibration for the encapsulated robotic implant.

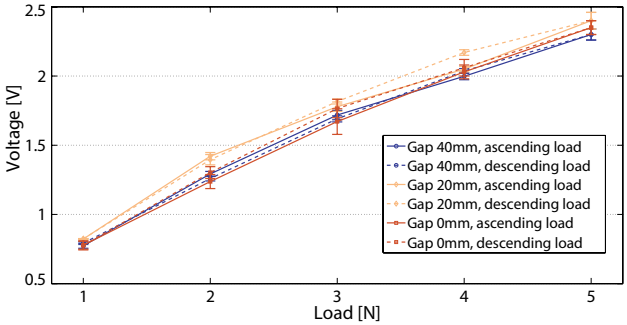

Fig. 9. Force sensor calibration for the encapsulated robotic implant.

the implant through its lower suture ring. The configuration shown is for the sensor calibration experiments. For tissue testing, the hanging weight was replaced with esophageal tissue as described later in this section.

A. Distance sensor calibration

Distance sensor calibration experiments were conducted on the encapsulated robotic implant. Three calibrated weights, 100, 200, and 300g, were attached to the lower suture ring as shown in Fig. 7. For each weight, the gap was set at distances of 40, 30, 20, and 10mm, in descending and ascending order, using a digital caliper. The output of the distance sensor acquired by the microcontroller was recorded.

Figure 8 depicts the sensor voltage with respect to the gap size. Four trials per condition were recorded (3 loads $\times$ 4 gaps $\times$ 2 directions $\times$ 4 trials = 96 trials in total). The average and standard deviation for each condition were computed over ten seconds of measurement. Based on this data, the gap between the suture rings is given by $G = -0.28V_G + 56.58$, ($R^2 = 0.99$) with a precision of ± 0.04V/mm, where G denotes the gap and V_G the voltage from the distance sensor.

B. Force sensor calibration

While the force sensor is not affected by transmission friction, the elastic force of the encapsulating sleeve may influence the transduced traction force. To produce a calibration curve, the experimental setup shown in Fig. 7 was used with ring gaps set at 40, 20, and 0mm using a digital caliper. At each gap, calibrated weights were applied ranging from 100 to 500g with a discretization step of 100g. The loads were attached to the lower suture ring in ascending and descending order. For each experimental condition, four trials were conducted (3 gaps $\times$ 5 loads $\times$ 2 directions $\times$ 4 trials = 120 trials in total). Each force signal was recorded for 40 seconds, and an average and standard deviation were computed over the last 20 seconds, when the signal was stable.

An approximately linear dependency exists between the load on the robotic implant's ring and the signal transduced by the incorporated force sensor, as shown in Fig. 9. The calibration curve is given by $F = 0.04V_F - 0.77$ with a precision of ± 0.004V/g, where F denotes the force and V_F represents the voltage output by the force sensor ($R^2 = 0.98$). Loads in the range of 1 to 5N are represented in a range of 0.80 to 2.35V.

C. Ex Vivo Experiments

In these experiments, fresh porcine esophagus (45kg animal) was mounted to the implant as shown in Fig. 10. Two tissue samples were used with lengths of 45 and 60mm. The inner and outer diameters of the two esophagi tissues were 9 and 14mm, respectively, which are similar in size to a normal human esophagus in a 3 months old patient (10-12mm when distended). Prior to experiments, the esophagus was kept in phosphate buffered saline (PBS) solution at 4° Celsius to preserve tissue properties. The esophagus tissue was mounted on the bottom suture ring of the robotic implant as shown. The tissue attachment was made using a horizontal running suture (4-0 Prolene sutures (Ethicon, Inc)), as shown in Fig. 10B. The lower end of the esophagus was fixed to the base of the testing platform through a modified eyebolt and "U" stiches (Fig. 10C). The total load on the suture ring, comprised of the tissue and the eyebolt was 18 and 21g.

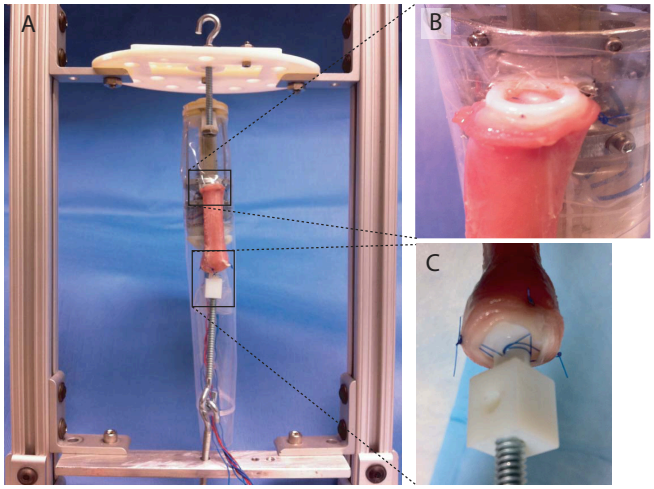

Fig. 10. Experimental setup for ex vivo tissue testing. A. Tissue is sutured to the lower ring of the robotic implant. B. Detail of tissue fixation to suture ring. C. Detail of fixation to platform base.

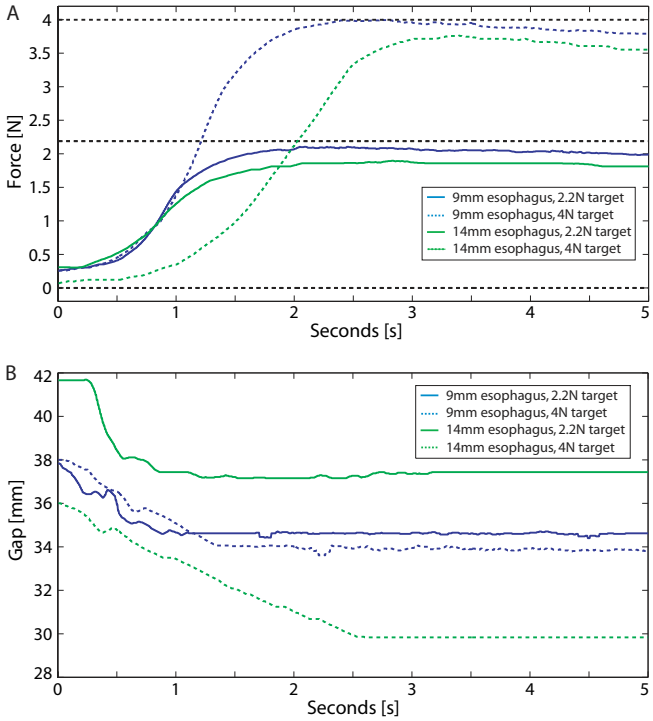

Fig. 11. Robotic implant response to step changes in traction force to 2.2 and 4N applied to two lengths of esophageal tissues. A. Force response. B. Displacement response.

The initial gap between the rings at the beginning of each experimental trial was approximately 40mm. At this position, the esophagi were set at a similar tension, maintaining their natural length. Each tissue was preconditioned before each trial by relaxing it for at least two minutes before exerting traction force. The moisture of the tissue was maintained by periodically wetting it with a fabric saturated with PBS.

For each experimental trial, the force controller was commanded to apply a traction force of either 2.2 or 4N. The measured force and displacement versus time are shown in Fig. 11. As desired, the robotic implant applies the targeted traction force in an overdamped manner (Fig. 11A), by decreasing the gap between the two rings (Fig. 11B). A slight gradual drop of the traction force was recorded by the force sensor suggesting that further tuning refinement of the controller may be needed. Initial and final displacements were verified with digital calipers. As can be expected the longer tissue sample requires more stretching to achieve a specified force.

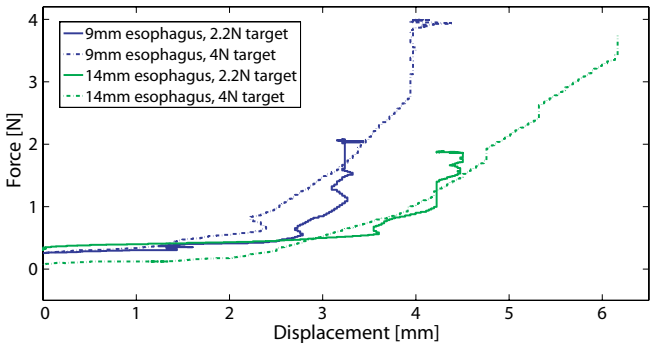

Fig. 12. Study of the tissue properties of two porcine animal esophagi.

Being equipped with both force and distance sensors, the robotic implant can also be used to investigate tissue properties, e.g., elasticity. To illustrate this, Fig. 12 plots the data from the previous figure as force versus displacement. These curves are comparable to the standard stress strain curves predicted for soft tissues [25] and also similar to those previously reported for ex vivo esophagus [26].

D. Energy demands

The maximum current drawn by the robotic implant during any given motor-on cycle was observed to be 0.2A. Considering that the robotic implant will be operated daily for up to 30 days and at most one minute per day to adjust traction force, the maximum cumulative power consumption is 100mAh. This value places the implant in the range of commercial polymer lithium ion batteries, suggesting the potential fur future wireless versions.

V. Conclusions

The paper introduces a tissue-traction robotic implant as a specific example of a new and unexplored class of medical robots. The initial prototype, sized for 2 year old patients, provides the necessary force production and control as well as sensing capabilities. Current research involves prototype size reduction to accommodate younger patients. Additionally, refinement of the implant design for in vivo studies is underway, which includes biocompatible encapsulation and extensive long-term controller tests. The studies based on the robotic implant can address not only current clinical shortcomings, but also provide the means to study the effect of force history on both tissue lengthening and tissue properties.

ACKNOWLEDGMENT

We thank Andrew Gosline and Christian Robles for their assistance in the development of the experimental setup.

REFERENCES

[1] B.J. Nelson, I.K. Kaliakatsos, and J.J. Abbott. Microrobots for minimally invasive medicine. *Annual Review of Biomedical Engineering*, 12:55–85, 2010.

[2] N. Patronik, M. A. Zenati T. Ota, and C. Riviere. A miniature mobile robot for navigation and positioning on the beating heart. *IEEE Transactions on Robotics*, 25(5):1109–1124, 2009.

[3] T. Ota, N. Patronik, D. Schwartzman, C. Riviere, and M. A. Zenati. Subxiphoid epicardial pacing lead implantation using a miniature crawling robotic device. *Journal of Surgical Research*, 137(2):242–243, 2007.

[4] M. E. Rentschler, S.M. Farritor, and K.D. Iagnemma. Mechanical design of robotic in vivo wheeled mobility. *Journal of Mechanical Design*, 129:1037–1045, 2007.

[5] P. Dario, M.C. Carroza, B. Lencioni, B. Magnani, D. Reynaerts, and M.G. Trivella et al. A microrobot for colonoscopy. In *Proceedings IEEE Seventh International Symposium on Micro Machine and Human Science*, pages 223–228, 1996.

[6] F. Carpi and C. Pappone. Magnetic maneuvering of endoscopic capsules by means of a robotic navigation system. *IEEE Transactions on Biomedical Engineering*, 56:14821490, 2009.

[7] M. Quirini, R.J. Webster III, A. Menciassi, and P. Dario. Design of a pill-sized 12-legged endoscopic capsule robot. In *IEEE International Conference on Robotics and Automation*, pages 1856 – 1862, 2007.

[8] X. Wang and M. Meng. A magnetic stereo actuation mechanism for active capsule endoscope. In *IEEE Engineering in Medicine and Biology Magazine*, pages 2811–2814, 2007.

[9] http://www.givenimaging.com.

[10] http://www.smartpillcorp.com.

[11] H.B. Kim, K. Vakili, B.P. Modi, M.A. Ferguson, A.P. Guillot, K.M. Potanos, S.P. Prabhu, and S.J. Fishman. A novel treatment for the midaortic syndrome. *New England Journal of Medicine*, 367(24):2361–2362, 2012.

[12] J.E. Foker, B.C. Linden, E.M. Boyle, and C. Marquardt. Development of a true primary repair for the full spectrum of esophageal atresia. *Annals of Surgery*, 226:4:533–543, 1997.

[13] J.E. Foker, T.C. Kendall Krosch, K. Catton, F. Munro, and K.M. Khan. Long-gap esophageal atresia treated by growth induction: the biological potential and early follow-up results. *Seminars in Pediatric Surgery*, 18:23–29, 2009.

[14] P.F. Martins Pinheiro, A.C. Sim oes e Silva, and R.M. Pereira. Current knowledge on esophageal atresia. *World Journal of Gastroenterology*, 18(28):3662–3672, 2012.

[15] M.M. Stone, E.W. Fonkalsrud, G.H. Mahour, J.J. Weitzman, and H. Takiff. Esophageal replacement with colon interposition in children. *Annals of Surgery*, 203(4):346–351, 1986.

[16] K.M. Bax. Jejunum for bridging long-gap esophageal atresia. *Seminars in Pediatric Surgery*, 18(1):34–39, 2009.

[17] A. Livaditis. Esophageal atresia: a method of over bridging large segmental gaps. *Z Kindershir*, 13:298–306, 1973.

[18] K. Kimura, E. Nishijima, C. Tsugawa, D.L. Collins, E.L. Lazar, S. Stylianos, A. Sandler, and R.T. Soper. Multistaged extrathoracic esophageal elongation procedure for long gap esophageal atresia: Experience with 12 patients. *Journal of Pediatric Surgery*, 36(11):1725 – 1727, 2001.

[19] S. Takamizawa, E. Nishijima, C. Tsugawa, T. Muraji, S. Satoh, Y. Tatekawa, and K. Kimura. Multistaged esophageal elongation technique for long gap esophageal atresia: experience with 7 cases at a single institution. *Journal of Pediatric Surgery*, 40(5):781–784, 2005.

[20] N. Tamburri, P. Laje, M. Boglione, and M. Martinez-Ferro. Extrathoracic esophageal elongation (kimuraś technique): a feasible option for the treatment of patients with complex esophageal atresia. *Journal of Pediatric Surgery*, 44(12):2420–2425, 2009.

[21] W.H. Hendren and J.R.Hale. Electromagnetic bougienage to lengthen esophageal segments in congenital esophageal atresia. *The New England Journal of Medicine*, 293(9):428 – 432, 1975.

[22] A. Oehlerking, D.P. Mooney, D.L. Trumper, J.D. Meredith, I.C. Smith, P.M. Nadeau, T. Gomez, and Z.A. Trimble. A hydraulically controlled nonoperative magnetic treatment for long gap esophageal atresia. *J. Med. Devices*, 5(2):027511, 2011.

[23] J.E. Foker, T.C. Kendall, K. Catton, and K.M. Khan. A flexible approach to achieve a true primary repair for all infants with esophageal atresia. *Seminars in Pediatric Surgery*, 14(1):8 – 15, 2005.

[24] M. Nagaya, J. Kato, N. Niimi, S. Tanaka, and K. Iio. Proposal of a novel method to evaluate anastomotic tension in esophageal atresia with a distal tracheoesophageal fistula. *Pediatric Surgery International*, 21(10):780–785, 2005.

[25] Y.C. Fung. Elasticity of soft tissues in simple elongation. *American Journal of Physiology*, 213(6):1532–1544, 1967.

[26] D. Sanchez-Molina, J. Velazquez-Ameijide, C. Arregui-Dalmases, V. Rodriguez, V. Quintana, M. Shafieian, and J.R. Crandall. A microcontinuum model for mechanical properties of esophageal tissue: Experimental methodology and constitutive analysis. *Annals of Biomed Engineering*, 42(1):62–72, 2014.